

Nonlinear thermal buckling behaviour of laminated composite panel structure including the stretching effect and higher-order finite element

Pankaj V. Katariya ^{1a}, Subrata K. Panda ¹ and Trupti R. Mahapatra ^{*2}

¹ National Institute of Technology Rourkela, Rourkela 769008, Odisha, India

² Veer Surendra Sai University of Technology (VSSUT), Burla 768018, Odisha, India

(Received February 28, 2018, Revised March 30, 2018, Accepted April 6, 2018)

Abstract. The nonlinear thermal buckling load parameter of the laminated composite panel structure is investigated numerically using the higher-order theory including the stretching effect through the thickness and presented in this research article. The large geometrical distortion of the curved panel structure due to the elevated thermal loading is modeled via Green-Lagrange strain field including all of the higher-order terms to achieve the required generality. The desired solutions are obtained numerically using the finite element steps in conjunction with the direct iterative method. The concurrence of the present nonlinear panel model has been established via adequate comparison study with available published data. Finally, the effect of different influential parameters which affect the nonlinear buckling strength of laminated composite structure are examined through numerous numerical examples and discussed in details.

Keywords: laminated composite curved panel; HSDT; Green-Lagrange strain; thermal buckling; FEM

1. Introduction

The development and subsequent advancement in the field of composite materials impersonated quite literally because of their unique lightweight and higher strength and stiffness properties including greater fatigue strength. This, in turn, increases the accessibility of the layered composite structure in the modern engineering (aeronautical, aerospace, automobile, sports and naval) industries where they are subjected to hostile environment under severe axial mechanical load while in service. The shear deformable laminated structures tend to buckle under couple thermomechanical loading. However, the buckling does not mean the final failure of the structure as the structure is capable of taking an extra amount of load after the geometrical distortion induced due to buckling known as its post-buckling strength. Hence, it is important from the designer's point of view to know the actual critical buckling load parameter and the corresponding post-buckling strength of layered structural component for their optimal design for subsequent application. As buckling is the geometrical instability of the structure due to the in-plane

*Corresponding author, Associate Professor, E-mail: truptiranjan01@gmail.com

^a Research Scholar, E-mail: pk.pankajkatariya@gmail.com

^b Associate Professor, E-mail: call2subrat@gmail.com

(mechanical, thermal and thermomechanical) loadings and can be modeled via the strain-displacement field. In general, the geometrical distortion associated with buckling is nonlinear in nature. Hence, the different kinds of strain fields (von-Karman and Green–Lagrange) in combination with various mid-kinematic theories are adopted by the designers for the exact modeling of the geometrical imperfection of the structural component.

Few articles are discussed in the following lines to establish the research gap from the earlier to the current day. Nath and Sandeep (1993) provided analytical solutions for the critical buckling and post-buckling responses of the laminated shallow spherical shell panel under uniformly distributed mechanical loading using Chebyshev series. The thermal critical buckling and the post-buckling loads of laminated composite plate are evaluated numerically using a four-node rectangular C1 continuous finite element (FE) by Singh and Rao (1993). Further, Reddy's higher-order shear deformation plate theory (HSDPT) in association with the perturbation technique is adopted by Shen (2000, 2001) for the evaluation of the buckling and post-buckling responses of the laminated plate structure under the uniform temperature and temperature dependant properties including the foundation effect (Nikrad et al. 2015). The post-buckling responses of laminated structure are investigated from time to time using the HSDPT, the first-order shear deformation plate theory (FSDPT) or the third-order shear deformation theory (TSDT) including von-Karman nonlinear strain field under the temperature or the combined thermomechanical loading (Shukla and Nath 2002, Thankam et al. 2003 and Girish and Ramachandra 2005, Asadi et al. 2015a, b, c, 2017a, b). Further, the modified feasible direction technique (MFD) adopted by Topal (2009) for the prediction of the optimized frequency and buckling load parameter of the laminated cylindrical shell panel using the FSDPT kinematics and the finite element method (FEM). Vosoughi et al. (2011) reported the thermal post-buckling strength of the composite skew plate structure using the FSDPT mid-plane theory and Green's strain field including von-Karman assumptions. Panda and Singh (2013) examined the thermal post-buckling responses of the shallow spherical panel structure numerically using the nonlinear FEM. They have adopted the HSDPT and Green-Lagrange strain field for the modeling of the layered structure. Similarly, the buckling and post-buckling responses of the laminated composite and the skew sandwich plate structure are investigated by Upadhyay and Shukla (2013) using von-Karman type nonlinear strain kinematics in the framework of the HSDPT. Also, the HSDPT kinematics in association with Green-Lagrange strain field has been implemented for the modeling and analysis of nonlinear modal values of the laminated curved panel structure by Singh and Panda (2014). Subsequently, the buckling and the post-buckling strength of the laminated composite structure are modeled using the various kinematic theories (FSDPT, HSDPT, layerwise theory and classical laminate theory) and the nonlinear strain kinematics (von-Karman and Green-Lagrange) for the inclusion of excess geometrical distortion (Duran et al. 2015, Nikrad and Asadi 2015, Baseri et al. 2016, Cetkovic 2016, Kandasamy et al. 2016, Katariya and Panda 2016, Namdar and Darendeliler 2017) with and without thermal environment. In general, most of the research articles are employed the FEM techniques for the evaluation of the geometrical instability either using their own computer code or the commercial FE tool (ANSYS/ABAQUS) under the influence of the elevated thermal environment.

From the review, it is understood that a considerable amount of research have already been published on the linear/nonlinear buckling strength of the layered structure under the influence of the mechanical and/or thermal loading with and without temperature dependent composite properties. Additionally, we also note that most of the composite models are based on von-Karman type of geometrical nonlinearity in the framework of the HSDPT/FSDPT mid-plane kinematics for

the inclusion of excess thermal distortion. However, studies related to the geometrically nonlinear buckling behavior of laminated structures incorporating the extension/stretching terms alongside full nonlinearity in Green-Lagrange sense and including all the nonlinear higher-order terms in the formulation is not yet reported. Based on the available research gap, the laminated structural model has been developed using a higher-order kinematics and Green-Lagrange strain field including all of the nonlinear higher-order terms. The structural equilibrium equation is obtained by minimizing the total potential energy functional in conjunction with the isoparametric finite element steps. The desired post-buckling strength are obtained numerically with the help a direct iterative method. Further, the model stability including the accuracy has been demonstrated by solving the different numerical examples. Finally, the effect of various geometrical parameters which influence the thermal post-buckling load is obtained computationally using the proposed numerical model and discussed in details.

2. Mathematical modeling

2.1 Geometry and displacement field

In the present study, the nonlinear buckling strength of the laminated composite flat and cylindrical shell panel composed of ‘ N ’ numbers of orthotropic layers of uniform thickness ‘ h ’ refer to Fig. 1. The shell panel dimensions utilized for the current analysis are length ‘ a ’, width ‘ b ’, and total thickness ‘ h ’. Additionally, ‘ R_x ’ and ‘ R_y ’ are the principal radii of the curvatures of the panel in their respective directions. It is assumed that the panel is stress-free at the constant temperature T_0 and the temperature rise, $\Delta T = T - T_0$, is uniform within the plate. The displacement field of laminated composite shell panel is considered based on the HSDPT mid-plane kinematics including the extension/stretching terms as in Katariya and Panda (2016)

$$\left. \begin{aligned} u(x, y, z, t) &= u_0(x, y, t) + z\theta_x(x, y, t) + z^2u_0^*(x, y, t) + z^3\theta_x^*(x, y, t) \\ v(x, y, z, t) &= v_0(x, y, t) + z\theta_y(x, y, t) + z^2v_0^*(x, y, t) + z^3\theta_y^*(x, y, t) \\ w(x, y, z, t) &= w_0(x, y, t) + z\theta_z(x, y, t) \end{aligned} \right\} \quad (1)$$

where, ‘ t ’ is the time, u , v and w are the displacement of any point within the panel along x , y and z directions, respectively. u_0 , v_0 and w_0 are the mid-plane displacement of any point within the panel along x , y and z directions, respectively. Similarly, θ_x , θ_y and θ_z are the rotation of normal to the mid-plane and extension terms, respectively along the corresponding directions. The functions u_0^* ,

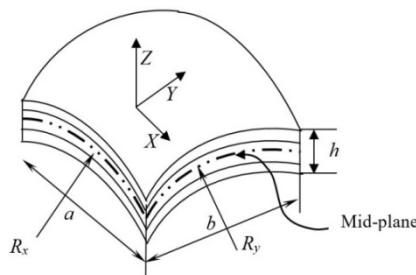


Fig. 1 Configuration of laminated composite shell panel

v_0^* , θ_x^* and θ_y^* are higher order terms of Taylor series expansion in the mid-plane of the shell panel.

2.2 Strain-displacement field

In order to consider the full geometric distortion, the nonlinear strain-displacement relation for the laminated composite shell panel is expressed based on Green-Lagrange type of nonlinearity as in Reddy (2004)

$$\{\varepsilon\} = \begin{Bmatrix} \varepsilon_{xx} \\ \varepsilon_{yy} \\ \varepsilon_{zz} \\ \gamma_{yz} \\ \gamma_{xz} \\ \gamma_{xy} \end{Bmatrix} = \begin{Bmatrix} \frac{\partial u}{\partial x} \\ \frac{\partial v}{\partial y} \\ \frac{\partial w}{\partial z} \\ \frac{\partial v}{\partial z} + \frac{\partial w}{\partial y} \\ \frac{\partial u}{\partial z} + \frac{\partial w}{\partial x} \\ \frac{\partial u}{\partial y} + \frac{\partial v}{\partial x} \end{Bmatrix} + \frac{1}{2} \begin{Bmatrix} \left[\left(\frac{\partial u}{\partial x} \right)^2 + \left(\frac{\partial v}{\partial x} \right)^2 + \left(\frac{\partial w}{\partial x} \right)^2 \right] \\ \left[\left(\frac{\partial u}{\partial y} \right)^2 + \left(\frac{\partial v}{\partial y} \right)^2 + \left(\frac{\partial w}{\partial y} \right)^2 \right] \\ \left[\left(\frac{\partial u}{\partial z} \right)^2 + \left(\frac{\partial v}{\partial z} \right)^2 + \left(\frac{\partial w}{\partial z} \right)^2 \right] \\ 2 \left[\left(\frac{\partial u}{\partial y} \right) \left(\frac{\partial u}{\partial z} \right) + \left(\frac{\partial v}{\partial y} \right) \left(\frac{\partial v}{\partial z} \right) + \left(\frac{\partial w}{\partial y} \right) \left(\frac{\partial w}{\partial z} \right) \right] \\ 2 \left[\left(\frac{\partial u}{\partial x} \right) \left(\frac{\partial u}{\partial z} \right) + \left(\frac{\partial v}{\partial x} \right) \left(\frac{\partial v}{\partial z} \right) + \left(\frac{\partial w}{\partial x} \right) \left(\frac{\partial w}{\partial z} \right) \right] \\ 2 \left[\left(\frac{\partial u}{\partial x} \right) \left(\frac{\partial u}{\partial y} \right) + \left(\frac{\partial v}{\partial x} \right) \left(\frac{\partial v}{\partial y} \right) + \left(\frac{\partial w}{\partial x} \right) \left(\frac{\partial w}{\partial y} \right) \right] \end{Bmatrix} \quad \text{or } \{\varepsilon\} = \{\varepsilon_l\} + \{\varepsilon_{nl}\} \quad (2)$$

The strain terms can be represented in terms of mid-plane strain terms by incorporating Eq. (1) in Eq. (2) as

$$\begin{aligned} \{\varepsilon_l\} + \{\varepsilon_{nl}\} = & \underbrace{\begin{Bmatrix} \varepsilon_x^{l_0} \\ \varepsilon_y^{l_0} \\ \varepsilon_z^{l_0} \\ \varepsilon_{yz}^{l_0} \\ \varepsilon_{xz}^{l_0} \\ \varepsilon_{xy}^{l_0} \end{Bmatrix} + z \begin{Bmatrix} 0 \\ k_y^{l_1} \\ k_x^{l_1} \\ k_{xy}^{l_1} \end{Bmatrix} + z^2 \begin{Bmatrix} 0 \\ k_{yz}^{l_2} \\ k_{xz}^{l_2} \\ k_{xy}^{l_2} \end{Bmatrix} + z^3 \begin{Bmatrix} 0 \\ k_{yz}^{l_3} \\ k_{xz}^{l_3} \\ k_{xy}^{l_3} \end{Bmatrix}}_{\varepsilon_L} + \frac{1}{2} \underbrace{\begin{Bmatrix} \varepsilon_x^{nl_0} \\ \varepsilon_y^{nl_0} \\ \varepsilon_z^{nl_0} \\ 2\varepsilon_{yz}^{nl_0} \\ 2\varepsilon_{xz}^{nl_0} \\ 2\varepsilon_{xy}^{nl_0} \end{Bmatrix} + z \frac{1}{2} \begin{Bmatrix} k_x^{nl_1} \\ k_y^{nl_1} \\ k_z^{nl_1} \\ 2k_{yz}^{nl_1} \\ 2k_{xz}^{nl_1} \\ 2k_{xy}^{nl_1} \end{Bmatrix}}_{\varepsilon_{NL}} + \\ & z^2 \frac{1}{2} \begin{Bmatrix} k_x^{nl_2} \\ k_y^{nl_2} \\ k_z^{nl_2} \\ 2k_{yz}^{nl_2} \\ 2k_{xz}^{nl_2} \\ 2k_{xy}^{nl_2} \end{Bmatrix} + z^3 \frac{1}{2} \begin{Bmatrix} k_x^{nl_3} \\ k_y^{nl_3} \\ k_z^{nl_3} \\ 2k_{yz}^{nl_3} \\ 2k_{xz}^{nl_3} \\ 2k_{xy}^{nl_3} \end{Bmatrix} + z^4 \frac{1}{2} \begin{Bmatrix} k_x^{nl_4} \\ k_y^{nl_4} \\ k_z^{nl_4} \\ 2k_{yz}^{nl_4} \\ 2k_{xz}^{nl_4} \\ 2k_{xy}^{nl_4} \end{Bmatrix} + z^5 \frac{1}{2} \begin{Bmatrix} k_x^{nl_5} \\ k_y^{nl_5} \\ k_z^{nl_5} \\ 2k_{yz}^{nl_5} \\ 2k_{xz}^{nl_5} \\ 2k_{xy}^{nl_5} \end{Bmatrix} + z^6 \frac{1}{2} \begin{Bmatrix} k_x^{nl_6} \\ k_y^{nl_6} \\ 0 \\ 0 \\ 0 \\ 2k_{xy}^{nl_6} \end{Bmatrix} \\ \text{or } \{\varepsilon_l\} + \{\varepsilon_{nl}\} = & [T^l] \{\bar{\varepsilon}_l\} + [T^{nl}] \{\bar{\varepsilon}_{nl}\} \end{aligned} \quad (3)$$

where, $[T^l]$ and $[T^{nl}]$ are the thickness co-ordinate matrix associated with the linear and nonlinear mid-plane strains and the details can be seen in Singh and Panda (2014). The terms $\{\bar{\varepsilon}_l\}$ and $\{\bar{\varepsilon}_{nl}\}$ are the mid-plane linear and nonlinear strain vectors and can be seen in Eq. (3).

2.3 Constitutive relation

The desired thermo-elastic constitutive relation of any arbitrary k^{th} layer of the orthotropic composite lamina is oriented at an arbitrary angle θ about any arbitrary axes are given by Jones (1999)

$$\{\sigma\}^k = [\bar{Q}]^k \left[\{\varepsilon_l\}^k - \{\alpha\}^k \Delta T + \{\varepsilon_{nl}\}^k \right] \tag{4}$$

where, $\{\sigma\}^k = \{\sigma_x \ \sigma_y \ \sigma_z \ \sigma_{yz} \ \sigma_{xz} \ \sigma_{xy}\}^T$, $\{\varepsilon\}^k = \{\varepsilon_x \ \varepsilon_y \ \varepsilon_z \ \varepsilon_{yz} \ \varepsilon_{xz} \ \varepsilon_{xy}\}^T$ and $[\bar{Q}]^k$ are the stress tensor, the strain tensor, and the reduced transformed stiffness matrix, respectively. Additionally, $\{\alpha\}^k = \{\alpha_1 \ \alpha_2 \ \alpha_{12}\}^T$ is the transformed thermal expansion coefficient vector for the k^{th} layer and the uniform temperature rise is denoted as ΔT .

Now, the thermal in-plane forces can be obtained by integrating the Eq. (4) over the thickness of the panel and can be expressed in the following mathematical form

$$\left\{ \{N_{\Delta}\}^T \quad \{M_{\Delta}\}^T \quad \{P_{\Delta}\}^T \right\} = \sum_{k=1}^N \int_{z_{k-1}}^{z_k} [\bar{Q}]^k \left\{ \begin{matrix} \alpha_1 \\ \alpha_2 \\ 2\alpha_{12} \end{matrix} \right\}^k \Delta T dz \tag{5}$$

where, $\{N_{\Delta}\}$, $\{M_{\Delta}\}$ and $\{P_{\Delta}\}$ are the resultant compressive in-plane membrane force vectors, moments and the higher order terms, respectively.

2.4 Strain energy of the laminate

The strain energy ($U_{S.E.}$) of the laminated composite shell panel can be expressed as

$$U_{S.E.} = \frac{1}{2} \int_V \{\varepsilon\}_i^T \{\sigma_i\} dV \tag{6}$$

By substituting the total strain and the stress tensors from the Eqs. (3) and (4) into the energy Eq. (6) and the final form of the energy functional of the panel configuration under uniform temperature loading expressed as

$$U_{S.E.} = \frac{1}{2} \int_V \{\varepsilon_i\}_i^k \left\{ [\bar{Q}]^k \left(\{\varepsilon_l\}^k - \{\alpha\}^k \Delta T + \{\varepsilon_{nl}\}^k \right) \right\}_i dV \tag{7}$$

2.5 Work done by the uniform temperature field

The total work done ($W_{\Delta T}$) by the in-plane thermal membrane force due to the influence of the uniform temperature rise (ΔT) of the curved laminated structural panel is computed using the Green-Lagrange type of strain field and expressed as

$$W_{\Delta T} = \frac{1}{2} \int_V \left[\begin{aligned} & \left[(\bar{u}_{,x})^2 + (\bar{v}_{,x})^2 + (\bar{w}_{,x})^2 \right] \{N_{\Delta x}\} + \\ & \left[(\bar{u}_{,y})^2 + (\bar{v}_{,y})^2 + (\bar{w}_{,y})^2 \right] \{N_{\Delta y}\} + \\ & 2 \left[(\bar{u}_{,x})(\bar{u}_{,y}) + (\bar{v}_{,x})(\bar{v}_{,y}) + (\bar{w}_{,x})(\bar{w}_{,y}) \right] \{N_{\Delta xy}\} \end{aligned} \right] dV \quad (8)$$

where, $\{N_{\Delta x}\}$, $\{N_{\Delta y}\}$ and $\{N_{\Delta xy}\}$ are the in-plane thermal force resultants per unit length.

The above work done expression as provided in Eq. (8) is linearized employing the procedure as given in Cook et al. (2000) and conceded as

$$W_{\Delta T} = \frac{1}{2} \int_A \{\varepsilon_G\}^T [D_G] \{\varepsilon_G\} dA \quad (9)$$

where, $\{\varepsilon_G\}$ and $\{D_G\}$ represents the geometric strain and the material property matrix, respectively due to the in-plane thermal loading.

2.6 Finite element formulation

FEM is widely appreciated numerical tool for the structural analysis of various geometrical and material complexities. In the present work, a nine-noded isoparametric element with ten DOFs per node is adopted for the discretization purpose. The displacement field of the present model expressed in terms of desired field variables. The displacement vector $\{\delta\}$ at any point on the mid-surface is given by

$$\{\delta\} = N_i \{\delta_i\} \quad (10)$$

where, $\{\delta_i\} = [u_{0_i} \ v_{0_i} \ w_{0_i} \ \theta_{x_i} \ \theta_{y_i} \ \theta_{z_i} \ u_{0_i}^* \ v_{0_i}^* \ \theta_{x_i}^* \ \theta_{y_i}^*]^T$ is the nodal displacement vector of the model and N_i is the interpolating function associated with node 'i'.

Now, substituting Eq. (10) into Eqs. (7) and (9) the strain energy and the work done expressions can be conceded as

$$U_{S.E.} = \frac{1}{2} \int_A \left(\begin{aligned} & \{\bar{\varepsilon}_l\}^T [D_1] \{\bar{\varepsilon}_l\} + \{\bar{\varepsilon}_l\}^T [D_2] \{\bar{\varepsilon}_{nl}\} + \\ & \{\bar{\varepsilon}_{nl}\}^T [D_3] \{\bar{\varepsilon}_l\} + \{\bar{\varepsilon}_{nl}\}^T [D_4] \{\bar{\varepsilon}_{nl}\} \end{aligned} \right) dA - \{F_{\Delta T}\}_i \quad (11)$$

$$[D_1] = \int_{-h/2}^{+h/2} [T^l]^T [Q] [T^l] dz, \quad [D_2] = \int_{-h/2}^{+h/2} [T^l]^T [Q] [T^{nl}]^T dz,$$

$$[D_3] = \int_{-h/2}^{+h/2} [T^{nl}]^T [Q] [T^l] dz, \quad [D_4] = \int_{-h/2}^{+h/2} [T^{nl}]^T [Q] [T^{nl}]^T dz$$

where

$$W_{\Delta T} = \frac{1}{2} \int_A \{\delta\}_i^T [B_G]_i^T [D_G] [B_G]_i \{\delta\}_i dA \quad (12)$$

The linear and nonlinear mid-plane strain vectors are rewritten in form of the nodal displacement vectors and mathematically expressed as

$$\{\bar{\epsilon}_l\} = [B]\{\delta\}, \{\bar{\epsilon}_{nl}\} = [A][G]\{\delta\} \tag{13}$$

where, $[B]$ linear strain-displacement matrix including the nodal shape functions and operator matrix. Whereas $[A]$ is the function of displacements associated with the nonlinear strain. Additionally, $[G]$ is the product form of differential operator and shape function in the nonlinear strain terms as same as the linear case. The details regarding the individual matrices can be seen in Singh and Panda (2014).

2.7 System of governing equation

The final form of the governing equation for the laminated shell panel is obtained by minimizing the energy expression and can be written as

$$\delta\Pi = 0 \tag{14}$$

where, $\Pi = (U_{S.E.} - W_{\Delta T})$.

Using Eqs. (7)-(14) the final governing equation of the system can be expressed as Panda and Singh (2013)

$$\left(([K_l] + [K_{nl}]) + T_{cr} [K_G] \right) \{\delta\} = 0 \tag{15}$$

Here, the force vector at right-hand side is zero and the effect of the temperature is considered in the geometric matrix $[K_G]$. The lowest eigenvalue, T_{cr} is the critical buckling temperature load. The $\{\delta\}$ is the global displacement vector, $[K_l]$ and $[K_{nl}]$ are the linear and the nonlinear global stiffness matrices, respectively. Further, the direct iterative procedure has been adopted for the solution of the Eq. (15) and the details regarding the implementation of nonlinear solution steps can be seen from the source (Panda and Singh 2013).

3. Results and discussion

After the development of the current higher-order nonlinear model and the corresponding computer code is further employed for the computation of results. The accuracy including the stability of the developed model established through the proper convergence and comparison. For the analysis purpose, the material properties are taken as same as Vosoughi et al. (2011) and provided i.e., $E_1/E_2 = 40$; $G_{12}/E_2 = 0.6$; $G_{13} = G_{12}$; $G_{23}/E_2 = 0.5$; $\nu_{12} = 0.25$; $\alpha_2/\alpha_1 = 10$, (where, ‘ E ’, ‘ G ’, ‘ ν ’, and ‘ α ’ are Young’s modulus, shear modulus, Poisson’s ratio, and coefficient of thermal expansion). For the computational purpose, the simply support end conditions are taken throughout the analysis, if not stated otherwise and represented as

$$v_0 = w_0 = \theta_y = \theta_z = v_0^* = \theta_y^* = 0 \quad \text{at} \quad x = 0, \quad a$$

$$u_0 = w_0 = \theta_x = \theta_z = u_0^* = \theta_x^* = 0 \quad \text{at} \quad y = 0, \quad b$$

Now, the convergence behaviour of the current numerical solutions are checked and compared with available published results. For the convergence, a square simply supported laminated composite plate responses are obtained using the present nonlinear model and presented in Fig. 2

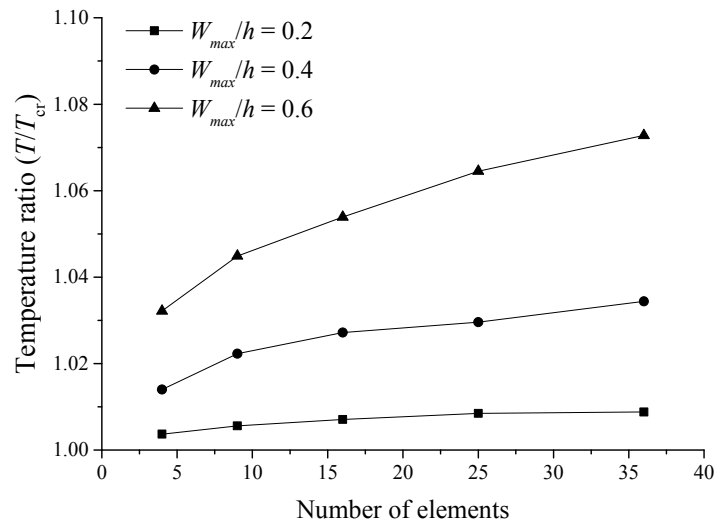


Fig. 2 Convergence study of the temperature ratio (T/T_{cr}) to different mesh division of a simply-supported square symmetric angle-ply $[\pm 45^\circ]_s$ laminated composite flat panel ($b/h = 30$)

Table 1 Comparison study of the temperature ratio (T/T_{cr}) of a simply-supported square symmetric angle-ply $[\pm 45^\circ]_s$ laminated composite flat panel ($b/h = 30$)

W_{max}/h	Present	Vosoughi et al. (2011)	Thankam et al. (2003)	Singh and Rao (1993)
	T/T_{cr}			
0.2	1.0088	1.0506	1.051	1.051
0.4	1.1344	1.2027	1.204	1.203
0.6	1.3728	1.457	1.459	1.459

for the different mesh divisions. From the responses, it is understood that the present results are converging well with the change in mesh sizes. The responses are computed by setting other related parameter i.e., three amplitude ratios ($W_{max}/h = 0.2, 0.4$ and 0.6), symmetric angle-ply $[\pm 45^\circ]_s$ lamination and the side-to-thickness ratio, $b/h = 30$ (where, W_{max} is the maximum central deflection of the panel structure). From the figure, it is understood that the responses are converging well with mesh refinement and 36 elements are sufficient to compute the responses, and the same is used throughout for the further analysis purpose.

Now, the present developed numerical model is validated by comparing the obtained results with the available published literature and presented in Table 1. For the computation purpose, the geometrical and material parameters are taken to be same as Vosoughi et al. (2011), and the responses are obtained for square symmetric angle-ply $[\pm 45^\circ]_s$ laminated composite flat panel. It is observed that the present results are as good as the reference values and the maximum difference is within 14%. It is important to mention that the difference arises between the present and reference results are due to the fact that the present model is developed using Green–Lagrange type of nonlinearity in the framework of the HSDT. In addition, the presently developed model includes all the nonlinear higher-order terms in the mathematical model that accounts for the original flexure of the shell panel structures more accurately.

3.1 Numerical examples

In this section, some new results are computed for the different geometrical parameters using the earlier defined support conditions and material properties to show the robustness of the present developed mathematical model. In this article, two different shell geometries viz. flat and cylindrical panels are analysed. The responses are computed for symmetric angle-ply ($[\pm 45^\circ]_S$) laminated composite shell panel and the effect of side-to-thickness ratios, curvature ratios ($R/a = 2, 5, 20, 50,$ and 100), aspect ratios ($a/b = 1, 1.5, 2,$ and 5) and amplitude ratios ($W_{max}/h = 0.2, 0.4, 1.0, 1.5,$ and 2.0) has been investigated to put forward few useful inferences.

3.1.1 Effect of side-to-thickness ratio

It is well known that the side-to-thickness ratio (b/h) increases than the structure become thin and it can be buckled easily. In order to investigate the effect, the nonlinear thermal buckling load responses of the square simply-supported angle-ply $[\pm 45^\circ]_S$ laminated composite flat and cylindrical panels are obtained using the various geometrical parameters. The responses are obtained using $b/h = 5, 10, 20, 30, 50,$ and $100, R/a = 20, W_{max}/h = 1.0$ and presented in Fig. 3. From the responses, it is observed that the nonlinear thermal buckling load decrease with increasing side-to-thickness ratio (b/h) which is a general case. This is because of the change in the stiffness of the structure, which affects the responses greatly. It is also noted that the differences in the buckling responses for different shell geometries (cylindrical and flat) are insignificant.

3.1.2 Effect of aspect ratio

It is well known that the aspect ratio of any structure is an important parameter to maintain the stable configuration. In addition, the structural stiffness is also significantly affected due to this. In this example, the effects of aspect ratio on the nonlinear thermal buckling load responses of the simply-supported angle-ply $[\pm 45^\circ]_S$ laminated composite flat and cylindrical panels has been investigated. For the computation purpose, the geometrical parameters are considered as $a/b = 1,$

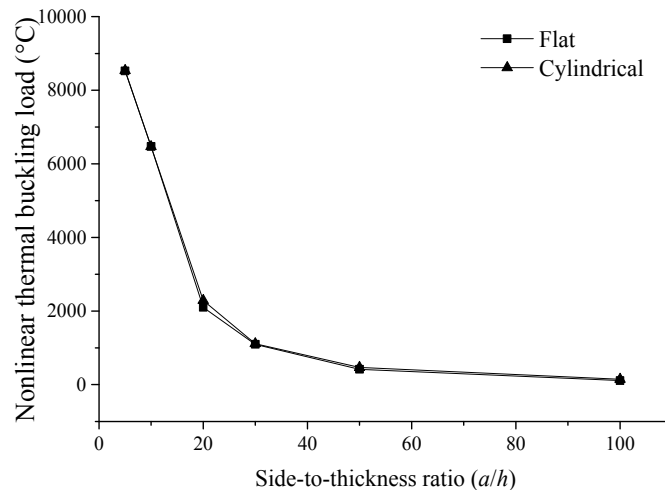


Fig. 3 Effect of side-to-thickness ratio (a/h) on nonlinear thermal buckling load of a square simply-supported symmetric angle-ply ($[\pm 45^\circ]_S$) laminated composite flat and cylindrical shell panel ($W_{max}/h = 1.0; R/a = 20$)

1.5, 2, and 5, $R/a = 20$, $b/h = 100$, $W_{\max}/h = 1.0$ and the responses are presented in Fig. 4. From the responses, it is observed that the nonlinear thermal buckling load decrease with an increase in the aspect ratio (a/b) which is expected and the reason behind this is the stiffness of the structure changes. However, it is worthy to note that the cylindrical panels show higher buckling load parameter in comparison to the flat panels irrespective of the aspect ratio values considered.

3.1.3 Effect of curvature ratio

Now, the effect of the curvature ratio (R/a) on the nonlinear thermal buckling load behaviour of the square simply supported angle-ply $[\pm 45^\circ]_s$ laminated composite cylindrical panel is studied. The responses are computed for the five curvature ratios, $R/a = 2, 5, 20, 50$, and 100 including $b/h = 100$ and $W_{\max}/h = 1.0$. The responses are plotted in Fig. 5. From the responses, it is observed that the nonlinear thermal buckling load decrease with an increase in the curvature ratio (R/a). This is because of the reduction in the overall structural stiffness of the panel structure, which decreases as the curvature ratio increases and as the curvature ratio increases the curved panel approaches to flat one, and the curved panels have higher membrane energy than the flat panels.

3.1.4 Effect of amplitude ratio

Various geometrical parameters have been considered to show the effect of the amplitude ratio (W_{\max}/h) on the nonlinear thermal buckling load of the square simply-supported angle-ply $[\pm 45^\circ]_s$ laminated composite flat and cylindrical panels. The responses are computed using $W_{\max}/h = 0.2, 0.4, 1.0, 1.5$, and 2.0 , $R/a = 20$, $b/h = 100$ and presented in Fig. 6. From the responses, it is observed that the nonlinear thermal buckling load increases with an increase in the amplitude ratio (W_{\max}/h). However, flat panels exhibit lower thermal buckling load parameters as compared to the cylindrical panels over the entire range of amplitude ratio values under consideration.

The nonlinear thermal buckling load parameter of the laminated composite shell panel structure is analysed in the present article. As a first step, a general mathematical model is developed based

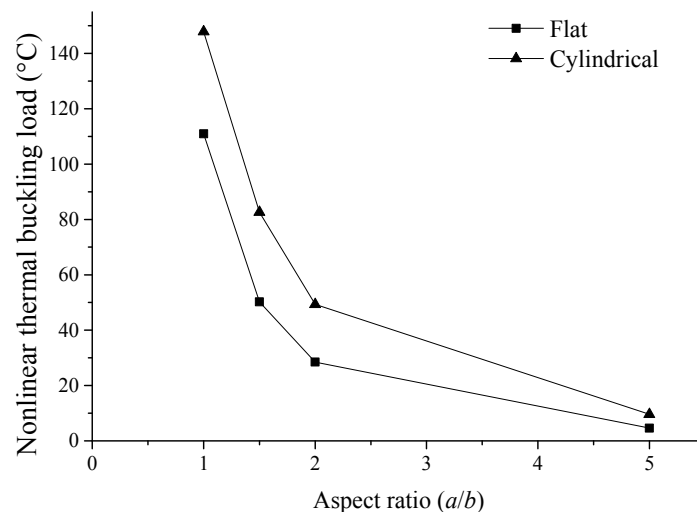


Fig. 4 Effect of aspect ratio (R/a) on nonlinear thermal buckling load of a simply-supported symmetric angle-ply ($[\pm 45^\circ]_s$) laminated composite flat and cylindrical shell panel ($W_{\max}/h = 1.0$; $b/h = 100$; $R/a = 20$)

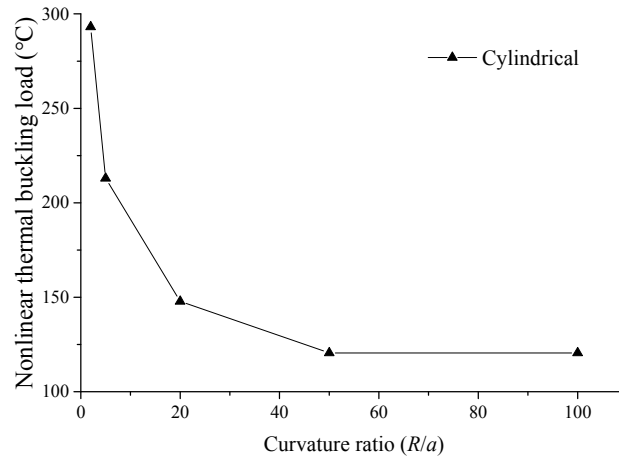


Fig. 5 Effect of curvature ratio (R/a) on nonlinear thermal buckling load of a square simply-supported symmetric angle-ply ($[\pm 45^\circ]_S$) laminated composite cylindrical shell panel ($W_{max}/h = 1.0$; $b/h = 100$)

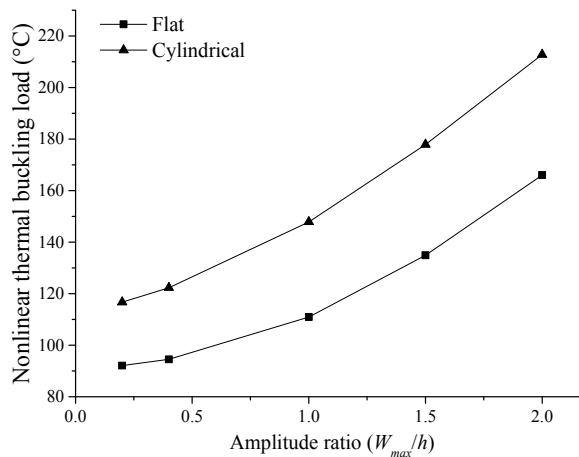


Fig. 6 Effect of amplitude ratio (W/h) on nonlinear thermal buckling load of a square simply-supported symmetric angle-ply ($[\pm 45^\circ]_S$) laminated composite flat and cylindrical shell panel ($b/h = 100$; $R/a = 20$)

on the higher-order kinematics for laminated flat/curved shell panel by considering the nonlinearity associated with geometry in Green–Lagrange sense. In addition to that, all the higher-order terms associated with the present nonlinear mathematical model are included in the formulation to obtain the exact behaviour of the structure. The differential governing equation of the laminated composite shell panel has been obtained using the finite element steps for the discretization purpose in conjunction with the direct iterative method. For the computational purpose, a generalized homemade computer code is developed in MATLAB environment based on the present mathematical model. Finally, few sets of numerical examples have been solved to bring out the effect of various geometrical parameters on the nonlinear thermal buckling load of the laminated composite shell panel structures and discussed in detail. The results indicate that, the

nonlinear thermal buckling load decrease with an increase in the side-to-thickness ratios, the aspect ratios as well as the curvature ratios whereas the nonlinear thermal buckling load increase with an increase in the amplitude ratios. This is because of the change in the stiffness of the structure, which affects the responses greatly.

4. Conclusions

The nonlinear thermal buckling load parameter of the laminated composite shell panel structure is analysed in the present article. As a first step, a general mathematical model is developed based on the higher-order kinematics for laminated flat/curved shell panel by considering the nonlinearity associated with geometry in Green–Lagrange sense. In addition to that, all the higher-order terms associated with the present nonlinear mathematical model are included in the formulation to obtain the exact behaviour of the structure. The differential governing equation of the laminated composite shell panel has been obtained using the finite element steps for the discretization purpose in conjunction with the direct iterative method. For the computational purpose, a generalized homemade computer code is developed in MATLAB environment based on the present mathematical model. Finally, few sets of numerical examples have been solved to bring out the effect of various geometrical parameters on the nonlinear thermal buckling load of the laminated composite shell panel structures and discussed in detail. The results indicate that, the nonlinear thermal buckling load decrease with an increase in the side-to-thickness ratios, the aspect ratios as well as the curvature ratios whereas the nonlinear thermal buckling load increase with an increase in the amplitude ratios. This is because of the change in the stiffness of the structure, which affects the responses greatly.

References

- Asadi, H. (2017a), “Numerical simulation of the fluid-solid interaction for CNT reinforced functionally graded cylindrical shells in thermal environments”, *Acta Astronaut.*, **138**, 214-224.
- Asadi, H., Souiri, M. and Wang, Q. (2017b), “A numerical study on flow-induced instabilities of supersonic FG-CNT reinforced composite flat panels in thermal environments”, *Compos. Struct.*, **171**, 113-125.
- Asadi, H., Kiani, Y., Shakeri, M. and Eslami, M.R. (2015a), “Exact solution for nonlinear thermal stability of geometrically imperfect hybrid laminated composite timoshenko beams embedded with SMA fibers”, *J. Eng. Mech.*, **141**(4), 04014144.
- Asadi, H., Akbarzadeh, A.H., Chen, Z.T. and Aghdam, M.M. (2015b), “Enhanced thermal stability of functionally graded sandwich cylindrical shells by shape memory alloys”, *Smart. Mater. Struct.*, **24**(4), 045022.
- Asadi, H., Kiani, Y., Aghdam, M.M. and Shakeri, M. (2015c), “Enhanced thermal buckling of laminated composite cylindrical shells with shape memory alloy”, *J. Compos. Mater.*, **50**(2), 243-256.
- Baseri, V., Jafari, G.S. and Kolahchi, R. (2016), “Analytical solution for buckling of embedded laminated plates based on higher order shear deformation plate theory”, *Steel Compos. Struct., Int. J.*, **21**(4), 883-919.
- Cetkovic, M. (2016), “Thermal buckling of laminated composite plates using layerwise displacement model”, *Compos. Struct.*, **142**, 238-253.
- Cook, R.D., Malkus, D.S., Plesha, M.E. and Witt, R.J. (2000), *Concepts and Applications of Finite Element Analysis*, John Wiley and Sons, Ltd., Singapore.
- Duran, A.V., Fasanella, N.A., Sundararaghavan, V. and Waas, A.M. (2015), “Thermal buckling of composite plates with spatial varying fiber orientations”, *Compos. Struct.*, **124**, 228-235.

- Girish, J. and Ramachandra, L.S. (2005), "Thermomechanical postbuckling analysis of symmetric and antisymmetric composite plates with imperfection", *Compos. Struct.*, **67**(4), 453-460.
- Jones, R.M. (1999), *Mechanics of Composite Materials*, Taylor & Francis, PA, USA.
- Kandasamy, R., Dimitri, R. and Tornabene, F. (2016), "Numerical study on the free vibration and thermal buckling behavior of moderately thick functionally graded structures in thermal environments", *Compos. Struct.*, **157**, 207-221.
- Katariya, P.V. and Panda, S.K. (2016), "Thermal buckling and vibration analysis of laminated composite curved shell panel", *Aircr. Eng. Aerosp. Tec.*, **88**(1), 97-107
- Nath, Y. and Sandeep, K. (1993), "Postbuckling of symmetrically laminated moderately thick, axisymmetric shallow spherical shells", *Int. J. Mech. Sci.*, **35**(11), 965-975.
- Namdar, O. and Darendeliler, H. (2017), "Buckling, postbuckling and progressive failure analyses of composite laminated plates under compressive loading", *Compos. Part B-Eng.*, **120**, 143-151.
- Nikrad, S.F. and Asadi, H. (2015), "Thermal postbuckling analysis of temperature dependent delaminated composite plates", *Thin-Wall. Struct.*, **97**, 296-307.
- Nikrad, S.F., Asadi, H., Akbarzadeh, A.H. and Chen, Z.T. (2015), "On thermal instability of delaminated composite plates", *Compos. Struct.*, **132**, 1149-1159.
- Panda, S.K. and Singh, B.N. (2013), "Thermal postbuckling behavior of laminated composite spherical shell panel using NFEM", *Mech. Based Des. Struct. Mach.*, **41**(4), 468-488.
- Reddy, J.N. (2004), *Mechanics of Laminated Composite: Plates and Shells - Theory and Analysis*, CRC Press, Boca Raton, FL, USA.
- Shen, H.S. (2000), "Thermomechanical postbuckling of imperfect shear deformable laminated plates on elastic foundations", *Comput. Method Appl. M.*, **189**(3), 761-784.
- Shen, H.S. (2001), "Thermal postbuckling behavior of imperfect shear deformable laminated plates with temperature-dependent properties", *Comput. Method Appl. M.*, **190**(40-41), 5377-5390.
- Shukla, K.K. and Nath, Y. (2002), "Thermomechanical postbuckling of cross-ply laminated rectangular plates", *J. Eng. Mech.*, **128**(1), 93-101.
- Singh, V.K. and Panda, S.K. (2014), "Nonlinear free vibration analysis of single/doubly curved composite shallow shell panels", *Thin Wall. Struct.*, **85**, 341-349.
- Singh, G. and Rao G.V. (1993), "Thermal post-buckling behavior of laminated composite plates", *AIAA Journal*, **32**(6), 1336-1338.
- Thankam, V.S., Singh, G., Rao, G.V. and Rath, A.K. (2003), "Thermal post-buckling behavior of laminated plates using a shear-flexible element based on coupled-displacement field", *Compos. Struct.*, **59**(3), 351-359.
- Topal, U. (2009), "Multiobjective optimization of laminated composite cylindrical shells for maximum frequency and buckling load", *Mater. Des.*, **30**(7), 2584-2594.
- Upadhyay, A.K. and Shukla, K.K. (2013), "Post-buckling behavior of composite and sandwich skew plates", *Int. J. Non Linear Mech.*, **55**, 120-127.
- Vosoughi, A.R., Malekzadeh, P., Banan, Mo.R. and Banan, Ma.R. (2011), "Thermal postbuckling of laminated composite skew plates with temperature-dependent properties", *Thin-Wall. Struct.*, **49**(7), 913-922.